Korean J. Chem. Eng., 35(4), 926-940 (2018)
DOI: 10.1007/s11814-017-0342-4

pISSN: 0256-1115
eISSN: 1975-7220

Plantwide design for high-purity formic acid reactive distillation process with dividing wall column and external heat integration arrangements

Felicia Januarlia Novita*, Hao-Yeh Lee,†, and Moonyong Lee*,†**

*School of Chemical Engineering, Yeungnam University, Dae-dong 38541, Korea
**Department of Chemical Engineering, National Taiwan University of Science and Technology, Taipei 10607, Taiwan
(*Received 31 July 2017 • accepted 12 December 2017*)

Abstract−We assessed eight configurations by implementing a dividing wall column (DWC) arrangement and an external heat integration (HI) arrangement for the reduction of energy consumption in the high-purity formic acid (FA) production process. At first, a patented high-purity FA production configuration was adopted and several main process variables were optimized. The optimal configuration was considered the base case for further investigation. The DWC arrangement was applied in the base case configuration to overcome the remixing phenomenon. Next, the external HI arrangement was implemented in those configurations. The simulation results showed that the non-reactive upper DWC between columns C2 and C3 with the HI configuration was the best configuration that provided 46.9% energy saving compared to base case configuration.

Keywords: Reactive Distillation, Dividing Wall Column, External Heat Integration, Energy Efficiency, Formic Acid Production

INTRODUCTION

Methanoic acid, also known as formic acid (FA), is an organic chemical raw material that has been utilized in many applications, such as involving leather tanning, pharmaceuticals/food chemicals, and textiles. High-purity FA is a necessity for most of such applications. The demand for FA has increased substantially since 2012 and is expected to increase [1]. According to the MarketsandMarkets homepage [2], the market price of FA is predicted to rise at a CAGR (compound annual growth rate) of 4.9% from 2014 to 2019 with a total estimated price of overall FA consumption $618,808,700 by 2019. Based on this report [2], FA is destined to be a profitable chemical to deal in the future.

Several processes have been explored for producing FA, each of which has its own advantages and disadvantages. One of the most common processes is the hydrolysis of methyl formate (MF), which is a more reasonable and economical process for FA production than others [3]. Huang et al. [4] applied a reactive distillation (RD) column in their patent to produce high-purity FA via hydrolysis of MF because of an azeotrope composition that needed to be broken down to obtain the high-purity FA. By implementing an RD column, less equipment was required for degrading the azeotrope composition that led to less cost incurred for achieving high-purity FA.

RD is an important example where two processes—reaction and separation—occur in a single column unit. The development and application of RD has received significant attention in the industry and academia [5]. A conversion rate increases in the RD column on removing the product, and separation is reduced by reacting away azeotropes. It is clear that RD can offer many advantages compared to the traditional reactor-separator system. Not only does it need less equipment, but it also offers improved yield, selectivity, and decreased energy requirement and also avoids hot spots [6]. Several publications have reported the importance of RD in industry. Over 100 important reaction systems using RD have been reported [7], suggesting that the implementation of RD in industry is important and promising in terms of energy and cost efficiency.

Another important issue of current interest in the field of process system engineering is intensification of the process by applying one or several promising methods and technologies so that higher economic benefits can be achieved. External heat integration (HI) arrangement is a promising method that offers an economic value when implemented in a process [8]. The economic benefit is realized when the latent heat of the overhead vapor stream from one column is transferred to the side or bottom reboiler of other columns [6]. However, the temperature limit has to be overcome so that the overhead temperature in one column must be sufficiently higher than the bottom temperature in another column. Otherwise, a side reboiler is needed as a heat sink.

Thermally coupled distillation (TCD) is another recommended technology to achieve lower energy consumption as a consequence of separation technologies that have improved continually. The basic principle of TCD is either the condenser or reboiler, or both, in one column being replaced by an interconnecting vapor liquid stream leading to other columns. TCD can save up to 30% of energy by reducing the remixing phenomenon that occurs in conventional distillation sequences [9-11]. Despite the reduction in energy consumption, there is a price to be paid when using thermally coupled systems. Operation is more difficult due to the large number of interconnections between columns. Therefore, it cannot be concluded

†To whom correspondence should be addressed.
E-mail: haoyehlee@mail.ntust.edu.tw, mynlee@yu.ac.kr

that complex configurations are always superior, compared with sequences of simple columns. Instead, the optimum configuration will be dependent on the specific mixture and feed conditions [12]. TCD can be considered thermodynamically equivalent to the dividing wall column (DWC) strategy if heat transfer from the divided wall is assumed negligible. The basic principle of DWC vertical wall involves the introduction of a column to divide the pre-fractionator and main column sections. Schultz et al. reported that the DWC can be an attractive alternative configuration for saving both energy and capital costs [13].

In process intensification (PI), RD and DWC are two of many possible routes to the advanced development of a conventional distillation unit [14]. Both represent two different ways of integration. However, RD and DWC can be combined to create a new process integration technique, termed the "reactive dividing wall column" (RDWC). The suitability of the RDWC for a particular reaction-separation system depends on various factors, such as the volatility of the reactants and products, reasonable reaction and distillation temperatures, and feedstock and product characteristics [15]. Several assumptions are required when building an RDWC [14]: (1) the mass-transfer resistances of all components are assumed equal by utilizing the height equivalent to a theoretical plate (HETP) value, and (2) heat transfer between the pre-fractionator and the main column through a vertical wall is negligible. In addition, no pressure drop influence on vapor distribution near a vertical wall due to vapor distribution below a vertical wall is treated ideally. By implementing an RDWC, the advantages of both integrated processes can be enhanced and further cost reduction is possible compared to the conventional distillation unit.

Based on the reaction zone, there are three RDWC configura-

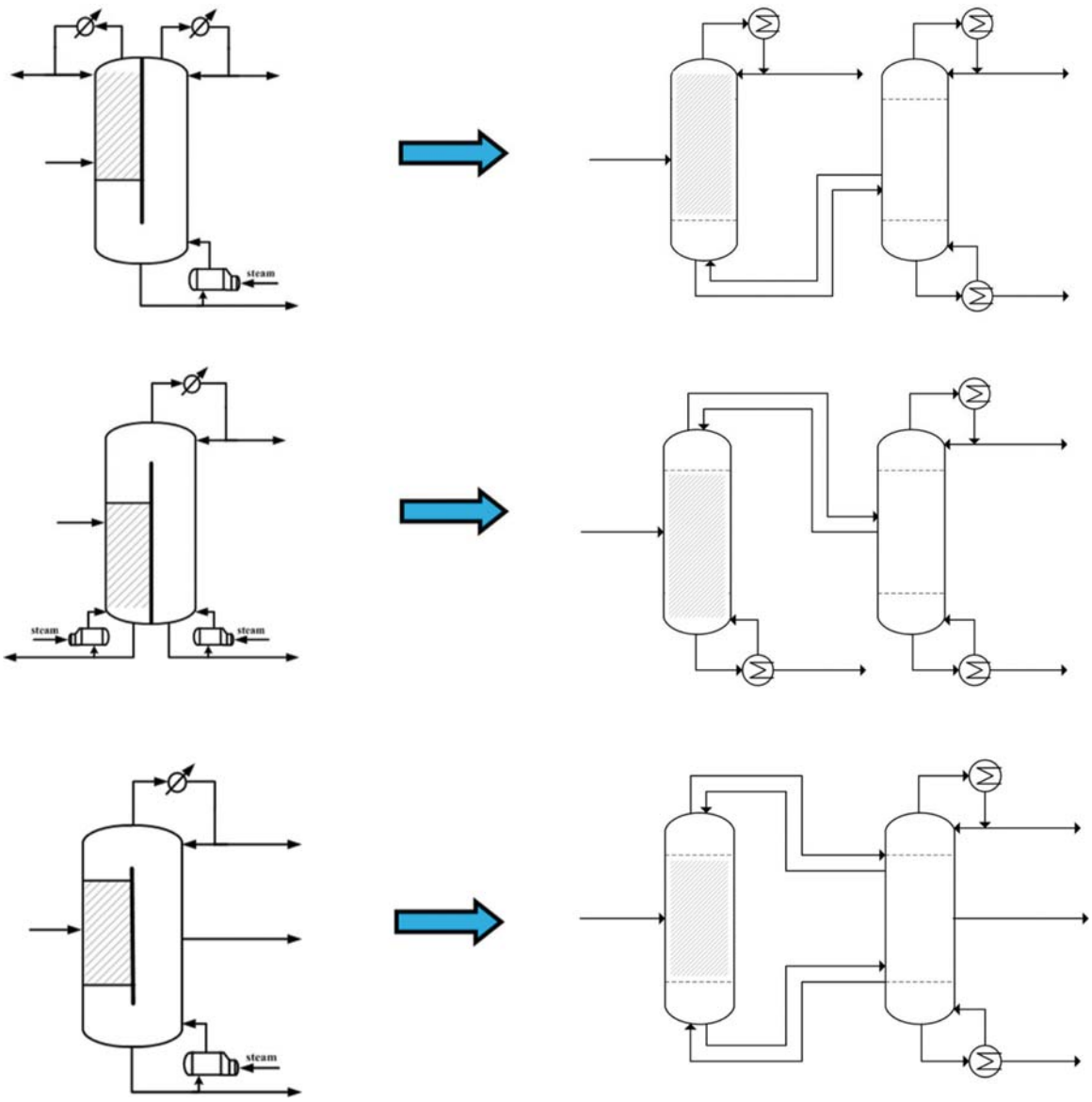

Fig. 1. The arrangement of RDWC thermodynamically equivalent to the thermally coupled configurations: (a) RDWC$_D$, (b) RDWC$_L$, and (c) RDWC$_M$.

tions (Fig. 1): (1) reactive upper DWC ($RDWC_U$), (2) reactive lower DWC ($RDWC_L$), and (3) reactive middle DWC (or $RDWC_M$).

The first arrangement, $RDWC_U$, removes one reboiler and changes it with an interconnecting vapor liquid stream, and a reactive zone exists in the top part of the column. This arrangement is thermodynamically equivalent to thermally coupled reactive distillation with a side rectifier ($TCRD_{SR}$). The second arrangement, $RDWC_L$, removes one condenser and changes it with an interconnecting vapor liquid stream and the reactive zone exists in the bottom part of the column. Thus, the $RDWC_L$ is thermodynamically equivalent to thermally coupled reactive distillation with a side stripper ($TCRD_{SS}$). The last arrangement, $RDWC_M$, which is thermodynamically equivalent to fully TCRD, removes one condenser and one reboiler and changes them with an interconnecting vapor liquid stream in each part and the reactive zone exists in the middle of the column.

In this study, we used a patented FA configuration proposed by Huang et al. [4] as the base case after an optimization procedure was completed. A commercial simulator, Aspen Plus V7.3, was used to conduct a rigorous simulation. The primary aim of this study was to examine the synergistic effects of a DWC arrangement and an external HI arrangement in high-purity FA production. The remixing phenomenon was used to illustrate the effect of DWC arrangement on the energy requirement. A side reboiler was needed in the external HI arrangement to handle the temperature limit for heat transfer.

REACTION KINETICS AND THERMODYNAMIC MODEL

In high-purity FA production, two reactions are involved. The first is a carbonyl reaction in an adiabatic continuous stirred tank reactor (CSTR) operating in a high-pressure condition. Eq. (1) represents the carbonyl reaction in this process:

$$CH_3OH+CO\leftrightarrow HCOOCH_3 \quad (1)$$

Two reactants, methanol (MeOH) and carbon monoxide (CO), react to produce methyl formate (MF). The catalyst used in this reaction can be a sodium methoxide (CH_3ONa) heterogeneous catalyst or an ion-exchange resin catalyst.

The second reaction is the MF hydrolysis reaction denoted by Eq. (2):

$$HCOOCH_3+H_2O\leftrightarrow HCOOH+CH_3OH \quad (2)$$

The MF hydrolysis occurs in the RD column. Two reactants, MF and water, react to produce formic acid (FA) and MeOH. The detailed kinetics of the carbonyl reaction and the hydrolysis reaction are provided in the Appendix.

In this study, data were fitted using the UNIQUAC thermodynamic model for the liquid phase and the Hayden-O'Connell (HOC) model for the vapor phase [6]. Details of the thermodynamic model are given in the Appendix.

PROCESS DESIGN AND OPTIMIZATION

As mentioned, the high-purity FA production process is referred to the patented process by Huang et al. [4]. Fig. 2 shows Huang et al's conceptual design to produce high-purity FA. First, the carbonyl reaction occurred in a high-pressure CSTR. MeOH and CO entered a CSTR that operated at 40 atm. The product of the carbonyl reaction was MF, which went to a flash unit together with the unreacted reactants. In the flash unit, the vapor product in the overhead stream was recycled back through a compressor to the CSTR and the liquid product in the bottom stream was sent to the first distillation column (column C1) that operated at 4 atm. In column C1, MF was separated from the unreacted MeOH, which was recycled back to the CSTR to increase the conversion rate of the CSTR. MF from the overhead stream of the C1 column was used as the main reactant for the second reaction; the MF hydrolysis reaction took place in the RD column. The operating pressure of the RD column was set at 4 atm and total reflux was applied for the condenser unit. A purge stream was used in the RD column to discharge the vaporized CO so that a very high pressure in the RD column could be prevented to ensure safety.

Then, the products of the MF hydrolysis reaction, FA and MeOH, were sent to the methanol separation column (column C2). MeOH, which is a distillate of column C2, was sent back to the CSTR for the same purpose as before, to increase the conversion rate in the

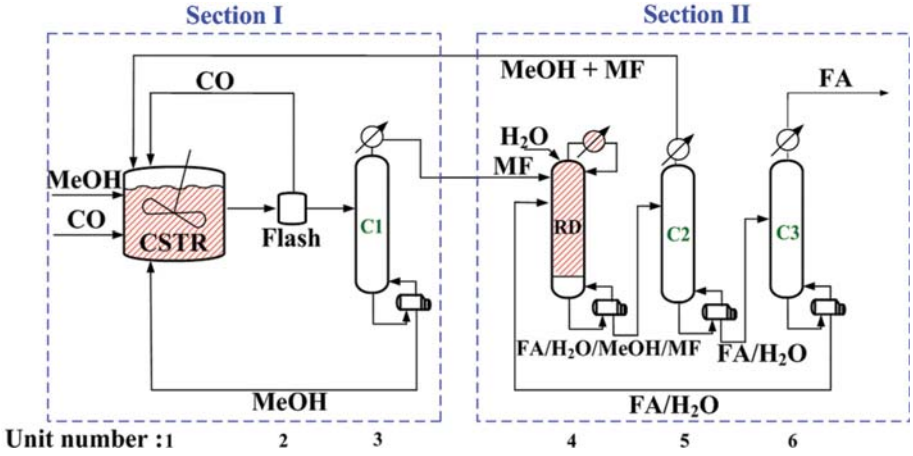

Fig. 2. Conceptual design of Huang et al to produce high-purity FA.

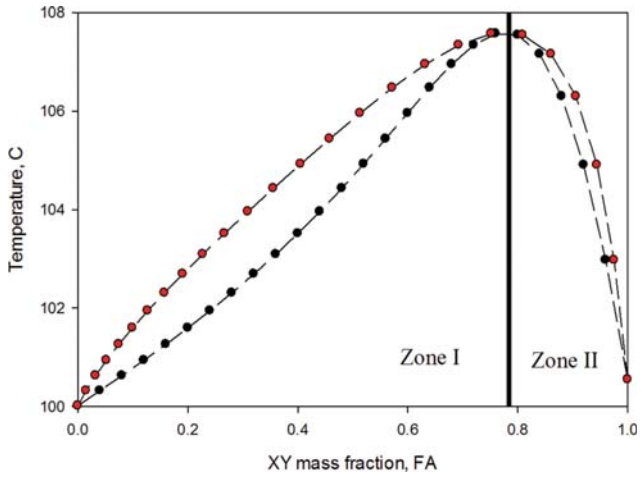

Fig. 3. T-x-y plot for the FA/water system.

CSTR. FA and unreacted water obtained in the bottom stream of column C2 were sent to the last distillation column (C3 column). FA and water formed an azeotrope, which needed to be considered while determining the column C3 feed composition to achieve high-purity FA. Fig. 3 shows the T-x-y plot for the FA/water system. According to Fig. 3, the feed composition for column C3 should be in zone II so that high-purity FA can be achieved as a distillate in column C3. Otherwise, the bottom product will contain an azeotrope.

Although the high-purity FA production process referred to Huang et al.'s patented work; however, many improvements were implemented in this study, such as several main process variables were optimized and a compressor unit was added. The high-purity FA production process was optimized by a mesh search method with four main process variables optimized: (1) mass fraction of MF distillate in column C1, (2) mass fraction of MF bottom product in the RD column, (3) mass fraction of methanol distillate in column C2, and (4) mass fraction of FA bottom product in column C3. Fig. 4 presents the sensitivity plots for these variables. The purity of each component can be met by varying the degree of freedoms of each column (i.e., the top composition of MF in column C1 can be met by varying the reflux ratio, the bottom product of MF in the RD column can be met by varying the reboiler duty of the RD column, the methanol distillate in column C2 can be met by varying the reflux ratio in column C2 and the FA bottom product in column C3 can be met by varying the reboiler duty of the column C3). The objective of this optimization procedure was to minimize the total reboiler duty of the four distillation columns (columns C1, C2, and C3 and the RD column).

As seen in Fig. 4, the optimal mass fraction of MF distillate in column C1 was found to be 0.78. A higher mass fraction of MF reaching the RD column will help the conversion rate in the column, which means that more FA can be generated. However, it will affect the energy needed for separation in column C1. A higher mass fraction of MF means higher energy requirements for column C1. Therefore, a mass fraction of 0.78 in the feasible range of 0.74-0.81 was found to be the optimal value. An amount of MF that remained in the RD column affected the performance of the

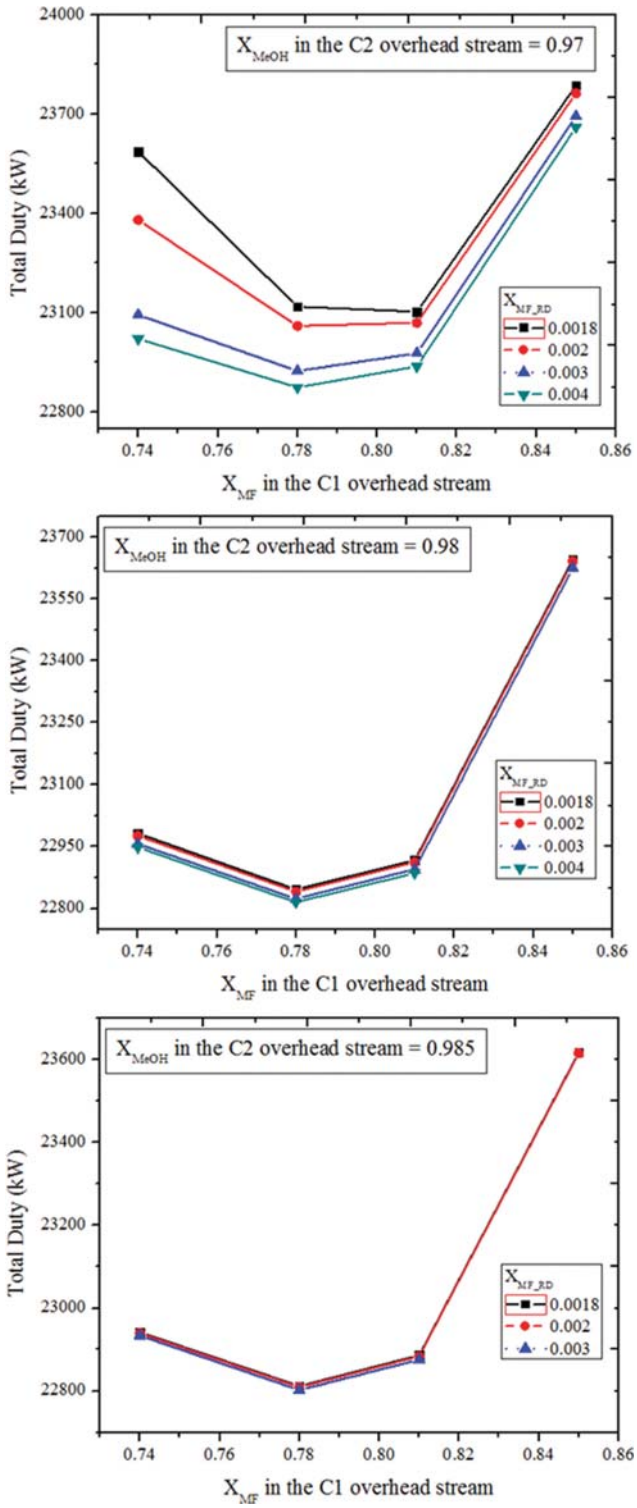

Fig. 4. Sensitivity plots for the optimization process variables for the high-purity FA production process.

column. The energy requirement was lower when more MF remained in the RD column. However, it resulted in a lower amount of FA product generated from the MF hydrolysis reaction. Less MF remained in the RD column, and more energy was required for the reaction-separation sequence, but a greater amount of FA

could be produced. A mass fraction of 0.003 MF in the bottom product of the RD column was found to present a good trade-off among the above advantages and disadvantages. A higher mass fraction of MeOH distillate in column C2 implied a higher energy requirement in the column. However, it affects the conversion rate in the CSTR so that it also affects the column C3 performance. The conversion rate in the CSTR increases and column C3 easily separates the components owing to their simple composition—only FA and water. The optimal mass fraction of MeOH distillate in column C2 was found to be 0.985. A mass fraction higher than 0.985 led to the divergence simulation. The lowest total reboiler duty was obtained when the mass fraction of the FA bottom product in column C3 was 0.86. A higher mass fraction of FA will increase the energy requirement of column C3 (data not shown). However, achieving a lower mass fraction of FA was impossible due to the formation of an azeotrope between FA and water. A mass fraction of 0.86 for FA was found to be the optimal mass fraction for the bottom product of column C3.

As a result, owing to the optimization process, the optimal high-purity FA production process was obtained. Fig. 5 displays a flowsheet for the optimal high-purity FA production process. This optimal configuration was used as the base case for further investigation. The objective of further investigation was to determine the total duty of reboiler for each column. However, the hydrolysis reaction section was the only one considered for further comparison because no large difference was noted for the carbonyl reaction section as a consequence of the RD feed composition being similar for all proposed configurations.

DIVIDING WALL COLUMN (DWC) ARRANGEMENTS

One arrangement that has been popular to decrease the energy consumption is the dividing wall column (DWC) through removal or reduction of the remixing phenomenon in the conventional distillation. In this study, DWC arrangement is proposed. However, due to the absence of a DWC model in Aspen Plus, a thermally coupled distillation (TCD) configuration is used as thermodynamically equivalent to DWC; for two columns in series, one reboiler/condenser was replaced by an interconnecting vapor liquid stream. Fig. 6 shows the liquid composition profiles of the RD column and columns C2 and C3 columns in the base case configuration.

Figs. 6(a) and 6(b) show the remixing phenomena occurring in the lower section of the RD column and column C2 respectively. Therefore, it is possible to introduce several optional arrangements. The investigation we undertook is explained in detail in the fol-

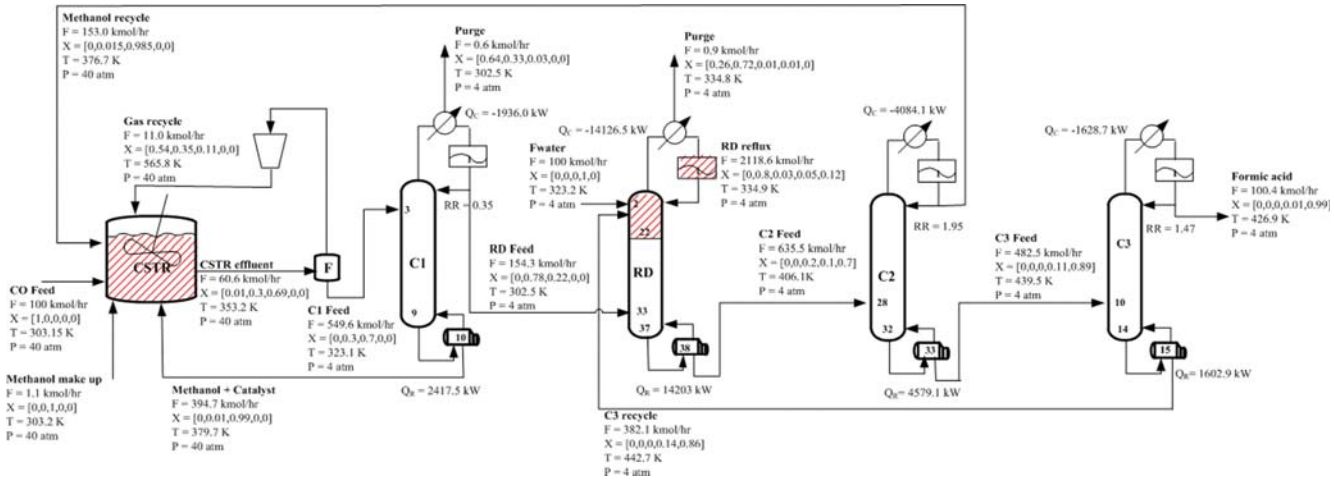

Fig. 5. Flowsheet of the optimal high-purity FA production process; X in X_{CO}, X_{MF}, X_{MeOH}, X_{H2O}, and X_{FA} denotes the mass fraction of the species.

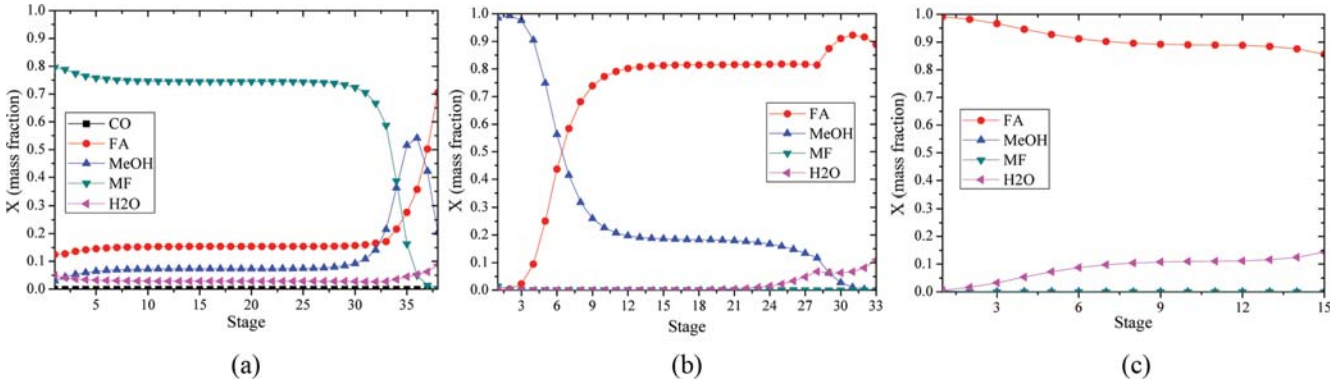

Fig. 6. Liquid composition profiles of the RD column (a) and columns C2 (b) and C3 (c) in the base case.

lowing sub-sections.

1. Reactive Upper DWC ($RDWC_U$) between RD Column and Column C2

The first DWC configuration proposed was the reactive upper DWC ($RDWC_U$) between the RD column and column C2. As shown in Fig. 6(a), an obvious remixing phenomenon mostly occurred in the lower section of the RD column. Therefore, on removing one reboiler in the RD column and implementing a vertical wall to divide the RD column and column C2, the remixing phenomenon is expected to be eliminated or at least reduced. It was assumed that no heat transfer occurred across a vertical wall [6] in this study for all proposed DWC arrangements. The DWC configuration was simulated on Aspen Plus utilizing an equivalent TCD configuration with a side rectifier. Fig. 7 shows the optimal $RDWC_U$ between the RD column and column C2.

To focus on the energy-saving effect of the configuration, the main structures (total number of stages and feed location) of columns in all proposed DWC arrangements were kept the same as those in the conventional configuration (base case). As optimization procedure in the conventional case, the mass fraction of FA in the bottom stream of column C3 for all proposed DWC arrangements has been optimized as well. Owing to the limited degree of freedom in the column for all proposed DWC arrangements (i.e., in column C3, the mass fraction of FA in the overhead stream was set by varying the reflux ratio and the mass fraction of FA in the bottom stream, which is C3 recycle stream, was set by varying the reboiler duty), the recycle flow rate (C3 recycle stream) was automatically determined. Therefore, all of the energy saving in the DWC arrangements was credited to the vapor side stream flow rate and the mass fraction of FA in the C3 recycle. The optimal mass fraction of FA in the bottom stream of column C3 was 0.8 mass fraction. While, the recycle flow rate observed of this configuration was 215 kmol/h. The reboiler duties of columns C2 and C3 were 15,142.4 kW and 2,390.8 kW, respectively, under the optimal condition of a vapor side stream of 1,287 kmol/h. As a result, the total duties of the RD column and column C2 decreased by around 3,639.7 kW on implementing an interconnecting vapor liquid stream between two columns. However, an increase of 787.9 kW could be observed for the duty of column C3 in this configuration, owing to a reduced amount of FA remaining in the recycled stream going into the RD column. This meant column C3 performed an extra separation task to obtain high-purity FA distillate in column C3.

Fig. 8 shows the liquid composition profile of the RD column, column C2 and column C3. The total reboiler duty decreased in this configuration because the remixing phenomenon in the lower section of the RD column had decreased (See Fig. 8(a)); 14% of the total reboiler duty was saved in the configuration with the $RDWC_U$ between the RD column and column C2, with a total reboiler duty of 17,533.1 kW.

2. Non-reactive Upper DWC ($NRDWC_U$) between Columns C2 and C3

As seen in Fig. 6(b), an obvious remixing phenomenon also occurred in the lower section of column C2. This phenomenon

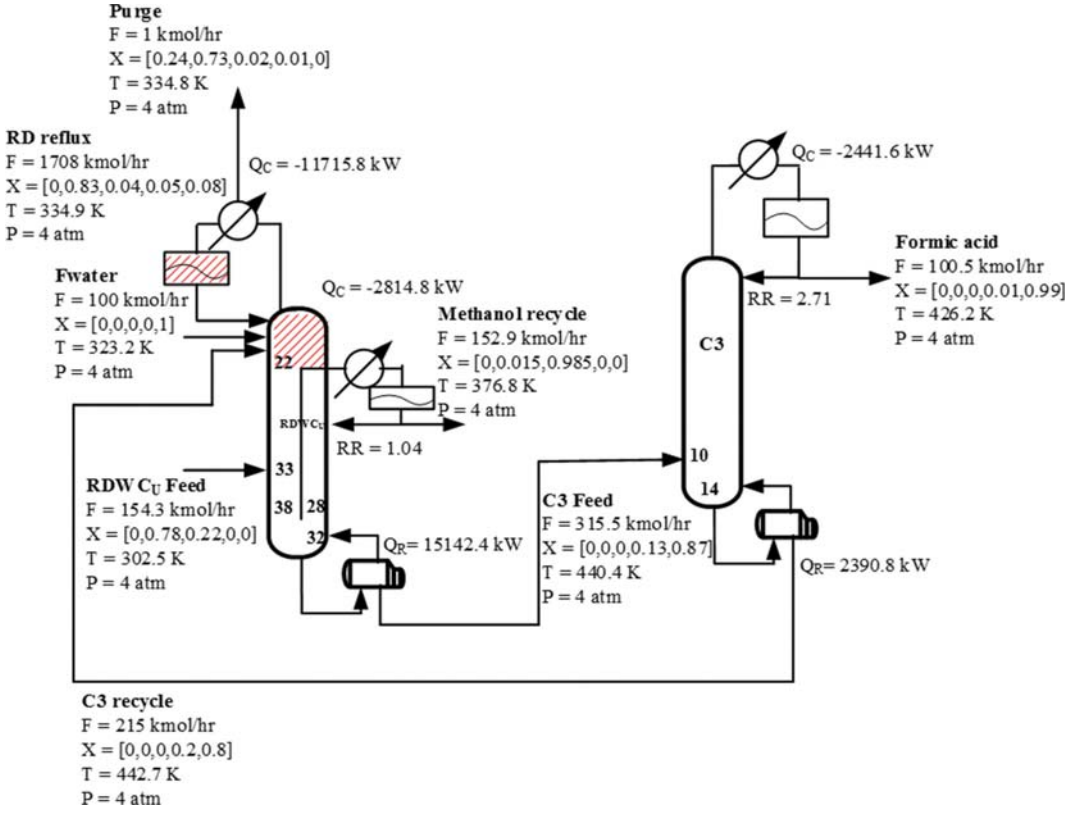

Fig. 7. Optimal $RDWC_U$ between the RD column and column C2, where X in X_{CO}, X_{MF}, X_{MeOH}, X_{H2O}, and X_{FA} denotes the mass fraction of the species.

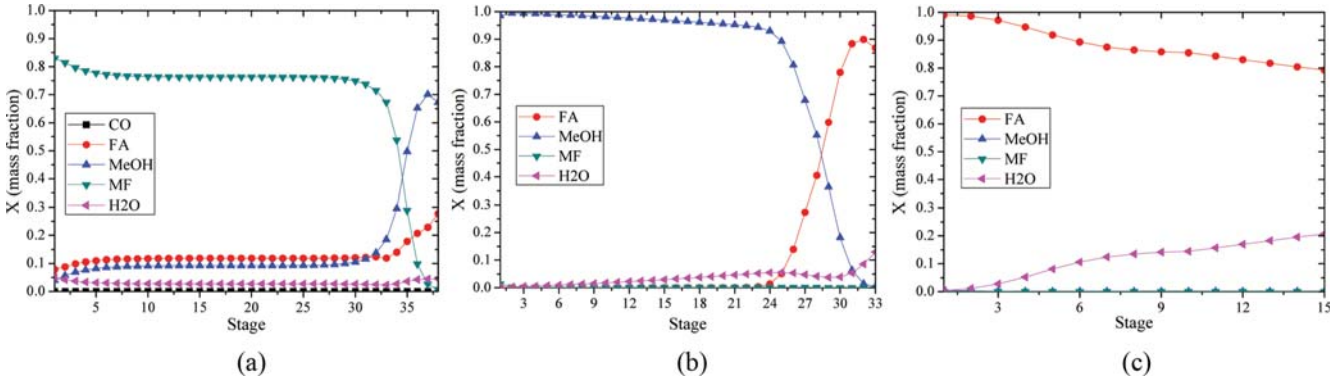

Fig. 8. Liquid composition profiles of the RD column (a), column C2 (b), and column C3 (c) in the configuration with RDWC$_U$ between the RD column and column C2.

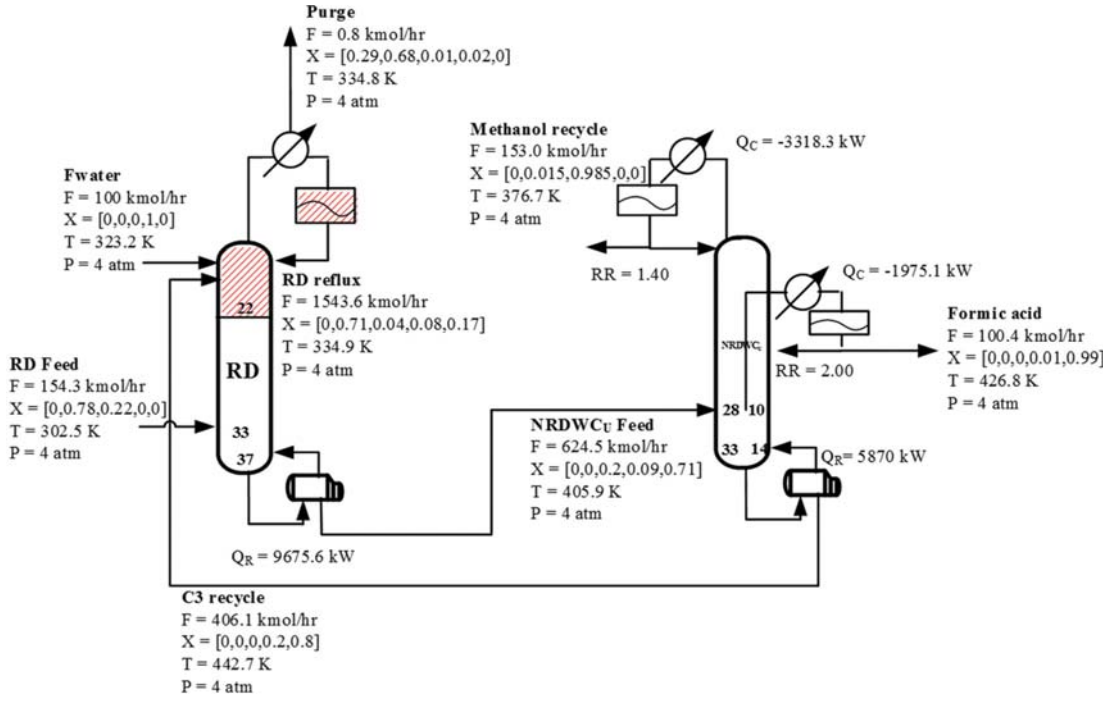

Fig. 9. Optimal NRDWC$_U$ between columns C2 and C3, where X in X_{CO}, X_{MF}, X_{MeOH}, X_{H2O}, and X_{FA} denotes the mass fraction of the species.

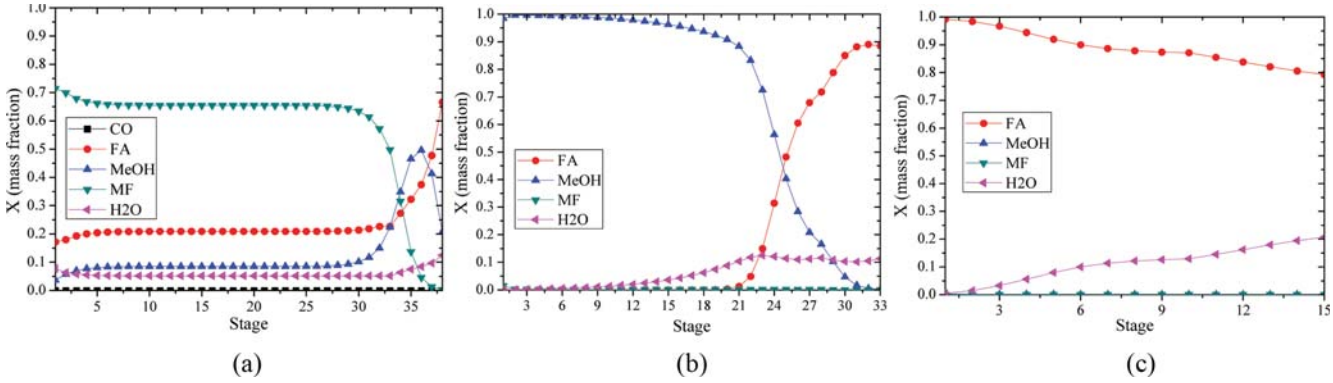

Fig. 10. Liquid composition profiles of the RD column (a), column C2 (b), and column C3 (c) in the configuration with NRDWC$_U$ between columns C2 and C3.

gave another option to implement the DWC between columns C2 and C3. One reboiler of column C2 was replaced by an interconnecting liquid vapor stream. Fig. 9 shows the proposed DWC configuration named NRDWC$_U$, applied between columns C2 and C3.

Fig. 10 shows the liquid composition profiles of the RD column and columns C2 and C3 in this configuration. The pattern of the composition profile in the C2 column was extremely different from Fig. 6(b). However, it could be clearly recognized that the remixing phenomenon in the lower section of column C2 was eliminated by the DWC arrangement between columns C2 and C3. This situation led to an improvement in the energy efficiency: 23.7% of the total reboiler duty could be saved. The reboiler duty in the RD column decreased by around 4,527.4 kW. The optimal mass fraction of FA in the C3 recycle was 0.8 mass fraction, and the recycled stream of this configuration was found at 406.1 kmol/hr. Eliminating the remixing phenomenon in the lower section of column C2 resulted in a decrease of around 5% in the total reboiler duties between columns C2 and C3.

3. Non-reactive Upper DWC (NRDWC$_U$) between RDWC$_U$ and Column C3

Fig. 11 shows the final proposed DWC arrangement in this study, where the DWC was implemented to three columns in series. This configuration is a combination of two previous configurations, where each reboiler in the RD column and column C2 is replaced by an interconnecting vapor liquid stream—one between the RD column and column C2 and another between columns C2 and C3. So, one reboiler remains in column C3 while there are two interconnecting vapor liquid streams in this configuration.

For this proposed arrangement, the reboiler duty of column C3 was 17,436.3 kW. It means around 2,948.7 kW of the three reboiler duties was reduced, which is equivalent to 14.5% energy saving compared to the base case configuration. The optimal mass fraction of FA in the bottom stream of column C3 was 0.86 mass fraction. While the recycle stream flow rate of this configuration was observed at 340.1 kmol/hr.

Fig. 12 shows the liquid composition profiles of the RD column and columns C2 and C3 in this configuration. The composition profile of the upper section in the RD column is the same as that of the base case. However, the remixing effect in the lower section of the RD column has decreased. The pattern of the composition profile in column C2 is a bit different due to the location of an interconnecting vapor liquid stream leading from/to column C2. According to Fig. 12(c), the composition profile of the 1st stage to the 12th stage in column C3 constantly demonstrated high-purity FA production (close to a 0.99 mass fraction). It means that the C3 column performed an extra separation step that affected the reboiler duty of the column.

4. Comparison of the Three Proposed DWC Configurations

Table 1 lists the duties of each configuration, the recycle flow rate in the proposed DWC configurations, and the percentage of energy saving for each proposed DWC configuration compared to the conventional configuration. As shown in Table 1, all the three proposed DWC configurations saved energy. The RDWC$_U$ be-

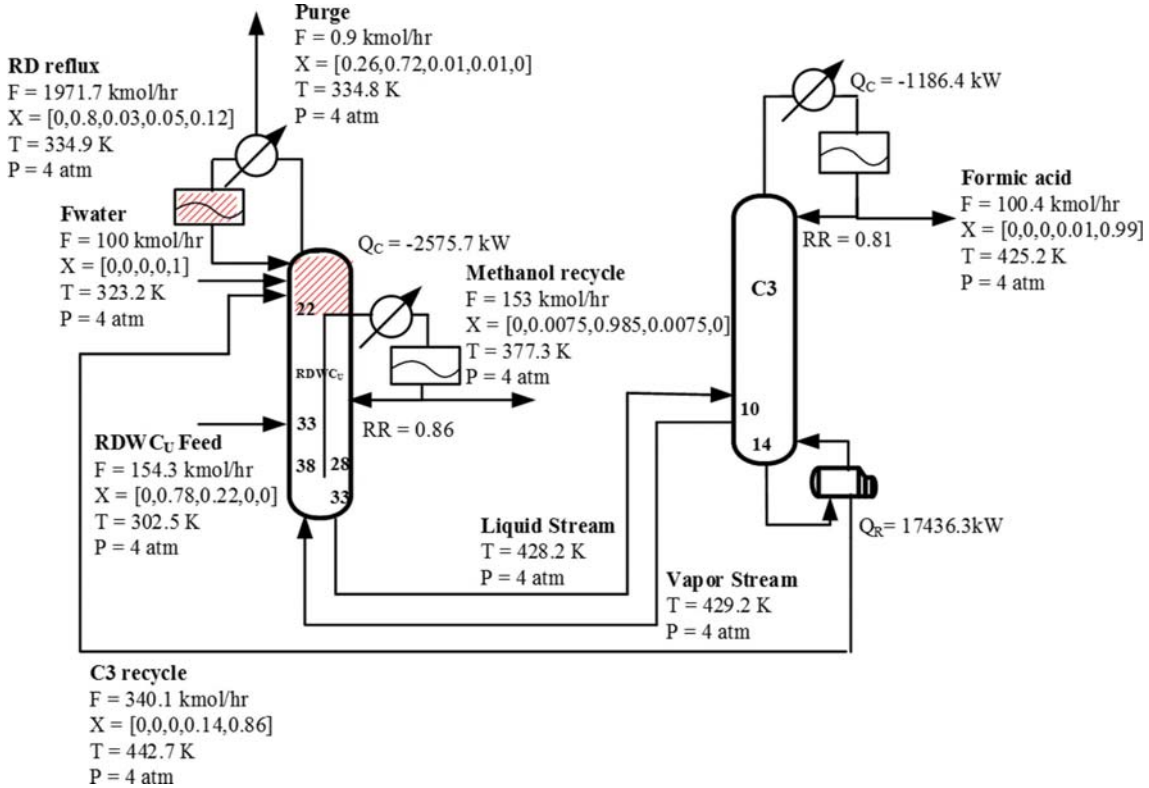

Fig. 11. Flowsheet for the configuration of the NRDWC$_U$ between the RDWC$_U$ and column C3, where X in X$_{CO}$, X$_{MF}$, X$_{MeOH}$, X$_{H2O}$, and X$_{FA}$ denotes the mass fraction of the species.

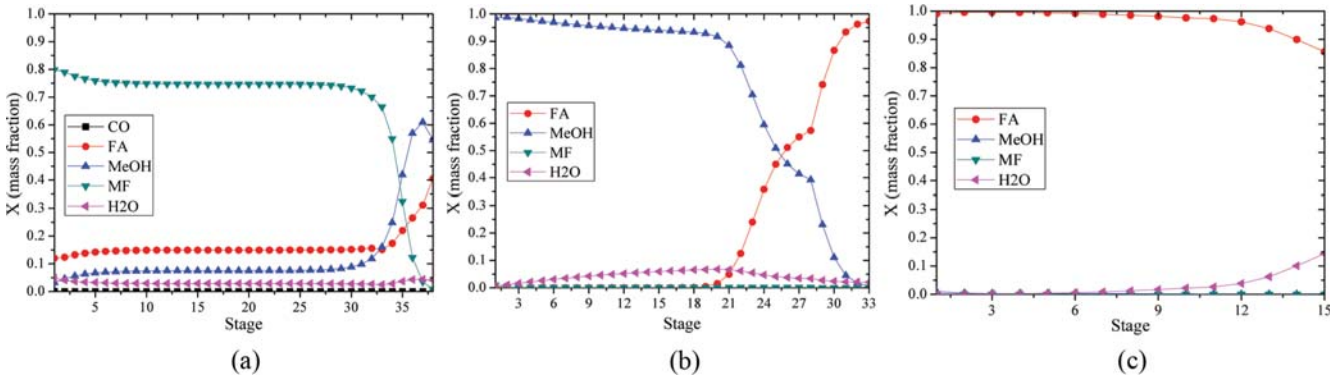

Fig. 12. Liquid composition profiles of the RD column (a), column C2 (b), and column C3 (c) in the configuration with the NRDWC$_U$ between RDWC$_U$ and column C3.

Table 1. Comparison of the conventional and proposed DWC configurations

RD reboiler duty (kW)	14203	-	9675.6	-
C2 reboiler duty (kW)	4579.1	15142.4	-	-
C3 reboiler dury (kW)	1602.9	2390.8	5870	17436.3
Total duty (kW)	20385.0	17533.1	15545.6	17436.3
Recycle flow rate in DWC case (kmol/h)	-	215.0	406.1	340.1
Energy saving (%)	-	14.0	**23.7**	14.5

tween the RD column and column C2 only saved around 14.0% energy. Meanwhile, the NRDWC$_U$ between columns C2 and C3 led to the highest energy saving of 23.7%. The NRDWC$_U$ between RDWC$_U$ and column C3, which was a combination of the two other configurations, did not obtain better results in terms of energy saving. This configuration only saved around 14.5% energy even though two DWCs were applied to three columns in series. The saving was comparable to that obtained by the RDWC$_U$ between the RD column and column C2.

The energy saving for the configuration with the NRDWC$_U$ between columns C2 and C3 was higher than that for the two other DWC configurations proposed. It might be observed that the large recycled amount appeared to contribute to the energy saving. Usually, a large recycle flow rate increases the energy requirement. However, the design results obtained for the three proposed DWC arrangements showed that the energy requirement decreased when the recycle flow rate increased. A higher energy efficiency was observed for a higher recycle flow rate, as shown in Table 1. This might occur as a result of higher conversion rate due to a higher recycle flow rate, which resulted in a lower energy requirement in the column. This observation implies that the DWC arrangement implemented in the process had an advantage in terms of energy efficiency owing to a decrease in the remixing phenomenon. As a result, the NRDWC$_U$ between columns C2 and C3 successfully achieved the highest energy saving among the proposed DWC configurations.

EXTERNAL HI ARRANGEMENTS

Another popular method to reduce the energy consumption is an external HI arrangement achieved by utilizing the latent heat of the overhead vapor stream of one column as the heat source of the other. However, a condition that needs to be considered when HI is applied is that the heat source temperature has to be sufficiently higher than that of the reboiler or heat sink in another column. When the temperature of the heat source is not sufficiently higher than that of the heat sink, several assisting configurations, such as a double-effect configuration or a heat-pump-assisted configuration, might help in handling the temperature limit. Such a configuration can be a suitable alternative to adding a side reboiler in the column so that neither a heat pump nor pressure change is needed [16].

In this study, we implemented external HI methods using a heat stream and/or a side reboiler. Fig. 13 shows the temperature profile of the RD column and columns C2 and C3 in the conventional base case configuration. The minimum temperature limit (ΔT_{min}) of 10 K was chosen for HI. As seen in Fig. 13, the temperature of the overhead section of column C3 was 20.8 K higher than the bottom temperature of the RD column. This means it was possible to transfer heat from the overhead vapor section of column C3 to the reboiler of the RD column. Thus, the first implementation of this application will address the effect of external HI arrangement on the conventional base case configuration.

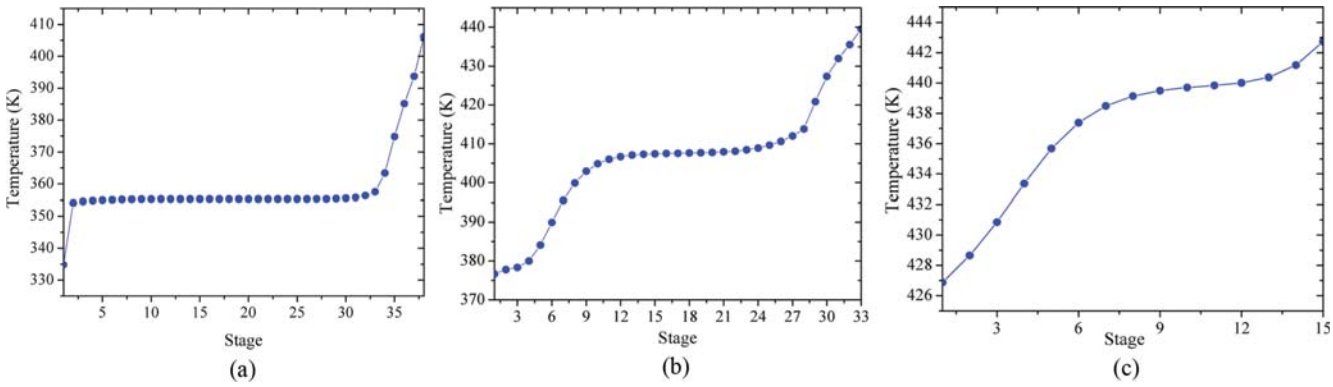

Fig. 13. Temperature profiles of the RD column (a) and columns C2 (b) and C3 (c) in the conventional base case configuration.

As shown in Figs. 5 and 13, there is room to implement an external HI arrangement in this configuration due to the sufficiently high latent heat obtained from the overhead section of column C2 (around 4,084.1 kW). The advantages of the external HI arrangement in this conventional base case configuration can be maximized by applying a side reboiler onto the RD column. The reason to implement a side reboiler is the temperature limitation between the RD column and column C2. The overhead temperature of column C2 was 376.7 K, which means the heat sink temperature should be at last 366.7 K to fulfill ΔT_{min}. Therefore, the appropriate location for the side reboiler implementation in this configuration was at the 31st stage. Fig. 14 presents the flowsheet for the proposed conventional base case with HI configuration.

As shown in Fig. 14, two external HI arrangements were applied in the configuration. The latent heat of the overhead vapor stream in column C3 was transferred to the bottom reboiler in the RD column by implementing a heat stream while that of the overhead vapor stream in column C2 was transferred to the side reboiler in the RD column. As a result, around 5,707.4 kW of duty in the RD column could be reduced. This HI saved 28% of the total energy requirement for three columns compared to the conventional base case without HI.

The heat stream can be illustrated as a model of a heat exchanger and its areas can be calculated using the following equation:

$$Q=AU\Delta T \tag{3}$$

where Q is the duty (kW), U is the overall heat transfer coefficient (kW/m^2·K), A is the area of the heat exchanger (m^2), and ΔT is the temperature difference between the column C3 condenser and the RD reboiler. The duty of this heat stream was 1,628.4 kW, the temperature difference was 20.8 K, and U was taken to be 0.568 kW/m^2·K, as cited in the report by Luyben [17]. As a result, the required area of the heat exchanger was calculated to be 137.83 m^2.

Thus, according to the conventional base case with HI arrangement, the external HI could provide good results in terms of reducing the energy consumption. The following sub-sections will investigate the implementation of the external HI arrangement in

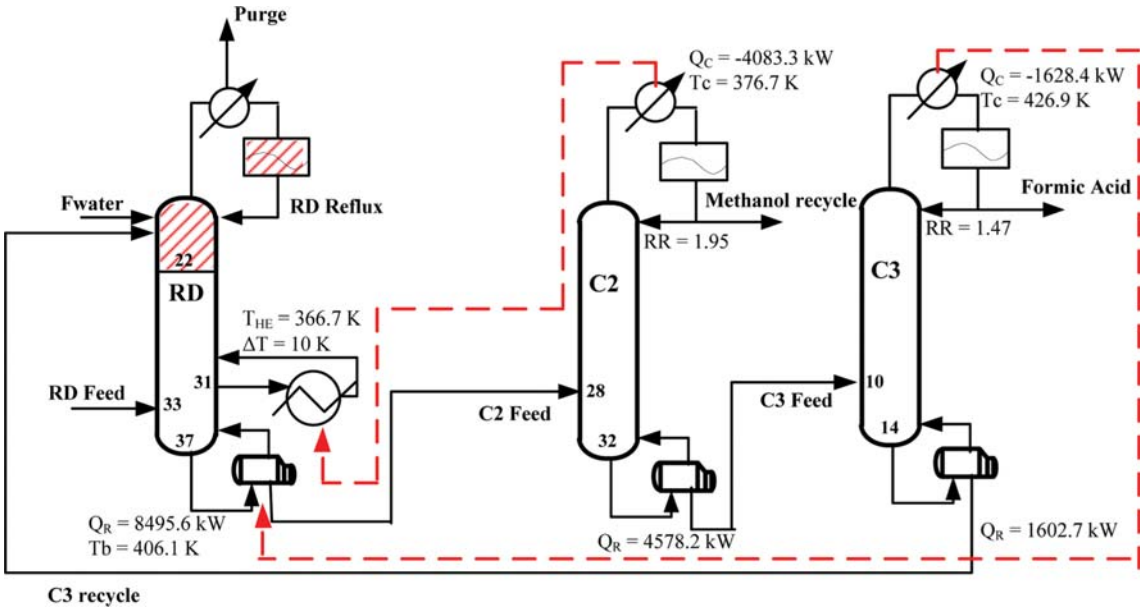

Fig. 14. Flowsheet for the conventional base case with HI via a side reboiler.

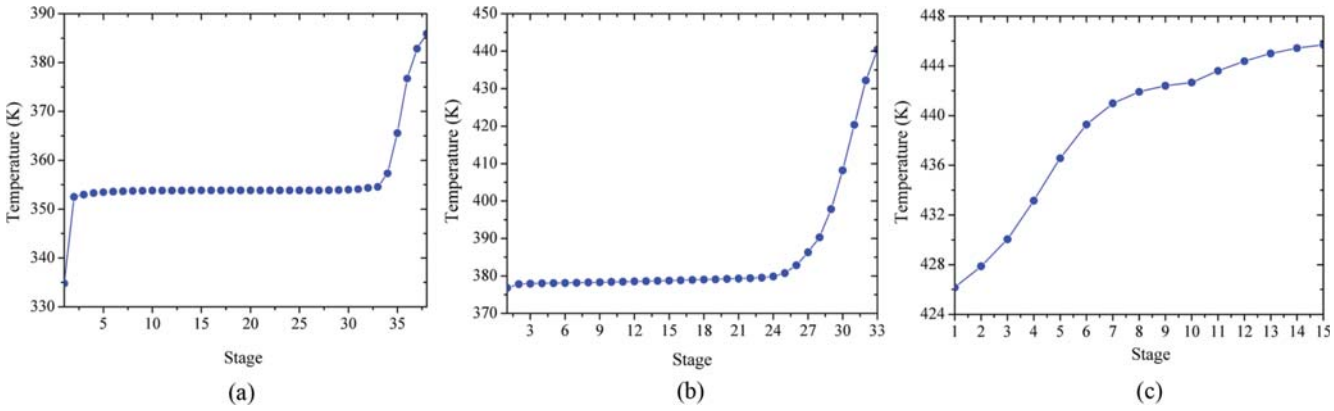

Fig. 15. Temperature profiles of the RD column (a) and columns C2 (b) and C3 (c) in the RDWC$_U$ between the RD column and column C2 configuration.

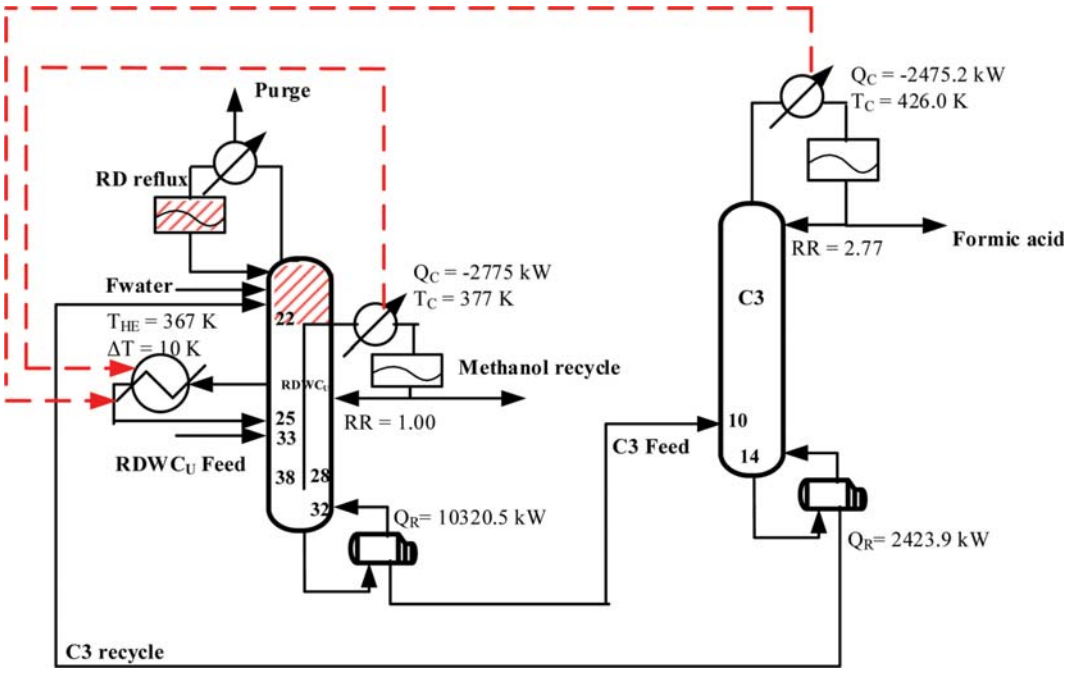

Fig. 16. Implementation of a side reboiler in the RDWC$_U$ between the RD column and column C2, representing external HI arrangement.

three proposed DWC arrangements. The purpose of this application was to consider synergistic effects between external HI and DWC arrangements toward energy efficiency for three columns in series.

1. RDWC$_U$ between the RD Column and Column C2 with HI Configuration

Fig. 15 shows the temperature profiles of the RD column and columns C2 and C3 in RDWC$_U$ between RD column and column C2 configuration. As shown in Fig. 7, there was no reboiler in the RD column for the RDWC$_U$ between the RD column and columns C2 and according to Fig. 15, the temperature of the overhead section in each column was lower than the temperature of the bottom section. Therefore, implementation of the external HI via a side reboiler could be an option for this configuration. Fig. 16 shows the flowsheet for configuration with the RDWC$_U$ between the RD column and column C2 with HI configuration.

In this configuration, the best location that gave the minimum total duty taking into account the ΔT_{min} constraint for a side reboiler was at the 25th stage. The latent heat of the overhead vapor stream from columns C2 and C3 was transferred to a side reboiler in the RD column. In this HI method, the bottom reboiler duty of column C2 could be reduced from 15,142.4 kW to 10,320.5 kW, which is equivalent to 31.8% energy saving compared to the configuration without HI. The overall energy requirement of this configuration with HI arrangement was 12,744.4 kW. The net energy savings made by the proposed configuration was 7,640.6 kW, which is equivalent to 37.5% energy savings compared to the conventional base case without HI.

2. NRDWC$_U$ between Columns C2 and C3 with HI Configuration

Fig. 17 shows the temperature profiles of the RD column and

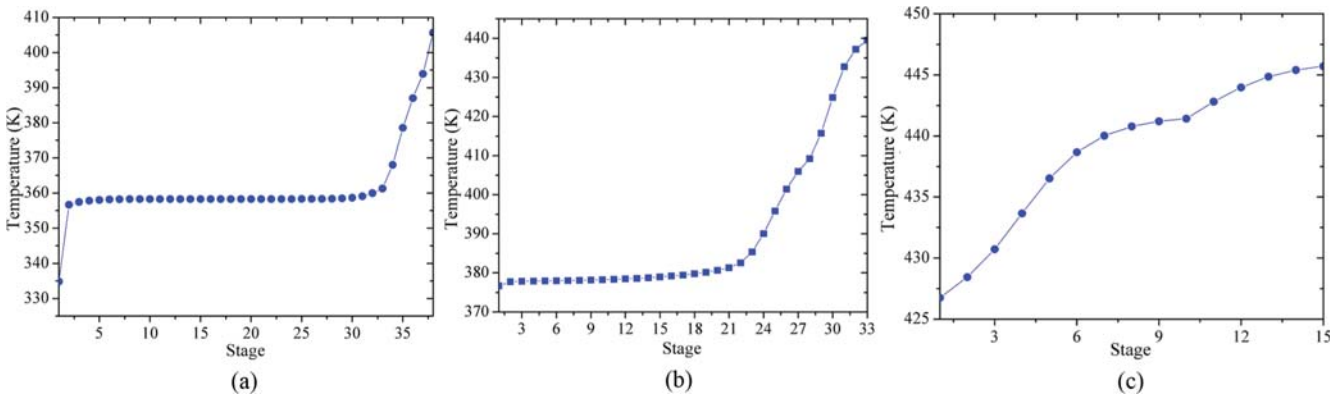

Fig. 17. Temperature profiles of the RD column (a) and columns C2 (b) and C3 (c) in the configuration with the NRDWC$_U$ between columns C2 and C3.

columns C2 and C3 in the configuration with the NRDWC$_U$ between columns C2 and C3. According to Fig. 17, the temperature of the overhead section in column C3 was 426.9 K, which was higher than the temperature of the bottom section in the RD column (405.9 K), but not higher than the overhead temperature of column C2 (376.7 K). Therefore, a side reboiler was added to the RD column to maximize the advantage of the external HI arrangement in this configuration. The heat sink temperature should be at least 366.7 K to fulfill ΔT_{min}. Therefore, the best location for the side reboiler implementation in this configuration was at the 24th stage. Fig. 18 represents the flowsheet for the proposed configuration with the NRDWC$_U$ between columns C2 and C3 with HI.

As shown in Fig. 18, the latent heat of the overhead vapor stream in column C3 was transferred to the bottom reboiler in the RD column by implementing a heat stream, while that of the overhead vapor stream in column C2 was transferred to the side reboiler in the RD column. This HI method is similar to the one implemented in the conventional base case with HI configuration. The only difference is the implementation of a DWC configuration between columns C2 and C3. In this HI method, the reboiler duty in the RD column could be reduced from 9,675.6 kW to 4,981.9 kW, which is equivalent to 48.5% energy saving compared to the proposed case involving the NRDWC$_U$ between columns C2 and C3 without HI. As a result, around 9,559.7 kW of total duties from three columns could be reduced compared to the conventional base case without HI configuration by implementing the synergistic effects between external HI and DWC arrangements. The percentage of the net energy saving owing to this configuration was calculated to be 46.9%. According to Eq. (3), if a heat stream that transferred heat from the overhead of column C3 to the bottom reboiler of the RD column was represented as a heat exchanger, then the required heat exchange area of the heat exchanger was 165.47 m^2.

3. NRDWC$_U$ between RDWC$_U$ and C3 Columns with HI Configuration

Fig. 19 shows the temperature profiles of the RD column and

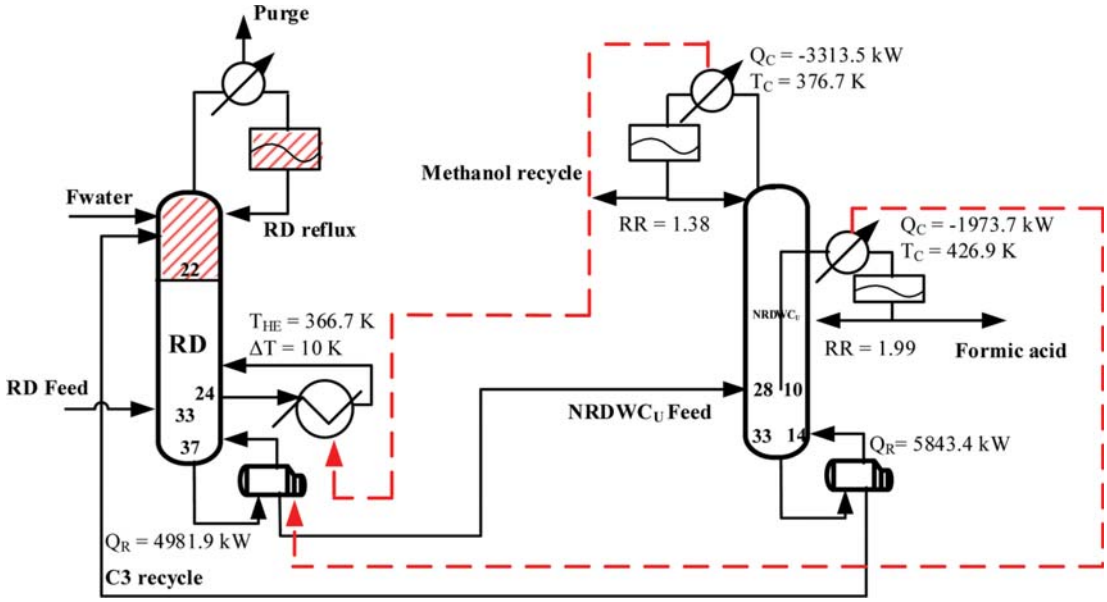

Fig. 18. Flowsheet for the proposed configuration with the NRDWC$_U$ between columns C2 and C3 with HI via a side reboiler.

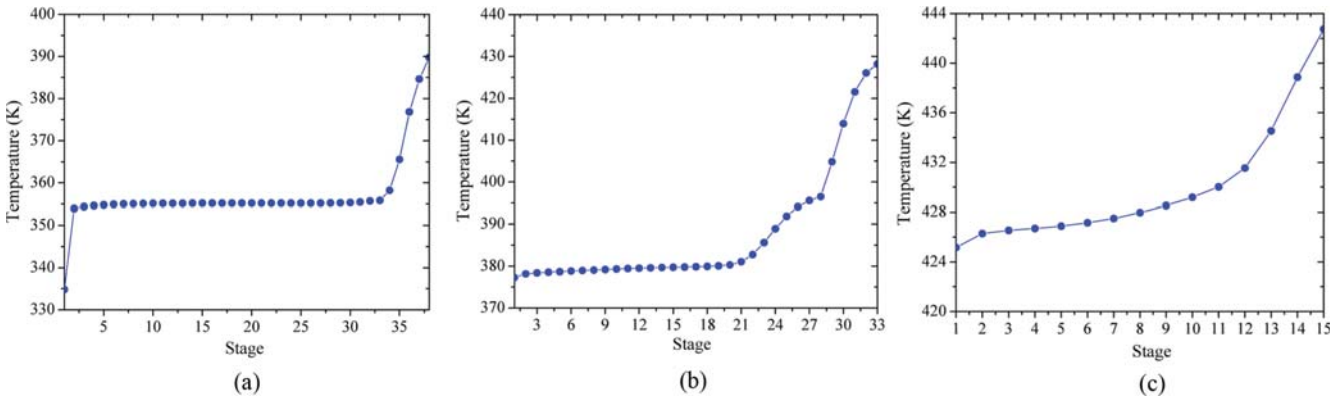

Fig. 19. Temperature profiles of the RD column (a) and columns C2 (b) and C3 (c) in the NRDWC$_U$ between RDWC$_U$ and column C3 configuration.

columns C2 and C3 in the configuration with the NRDWC$_U$ between RDWC$_U$ and C3 columns. As shown in Fig. 10, no reboiler was used in the RD column. Therefore, the implementation of an external HI arrangement in this configuration will be similar to that in the RDWC$_U$ between the RD column and column C2 with HI configuration. The difference in this configuration was the appropriate stage for the side reboiler that was at the 31st stage in the RD column. Fig. 20 shows the flowsheet for the implementation of a side reboiler in this configuration, representing the external HI arrangement.

The latent heat of the overhead vapor stream from columns C2 and C3 was transferred to a side reboiler in the RD column. In this HI method, the overall duties decreased from 17,436.3 kW to 14,201.6 kW, which is equivalent to 18.55% energy saving compared to the proposed configuration without HI. By implementing the synergistic advantages between external HI and DWC arrangements, this configuration could save 30.3% energy compared to the conventional base case without HI configuration.

4. Comparison of the Three Proposed DWC with HI Configurations

Table 2 lists the results obtained for all configurations with external HI arrangement.

As seen in Table 2, the conventional with HI configuration could save 28.0% energy compared to the base case (conventional without HI configuration). Among three DWC with the HI configurations, the proposed NRDWC$_U$ between columns C2 and C3 with the HI saved the most energy (46.9%) compared to the base case. While compared to the conventional with HI configuration, the proposed NRDWC$_U$ between columns C2 and C3 with the HI could save 26.2% of energy. The two other configurations, the RDWC$_U$ between the RD column and column C2 configuration and the NRDWC$_U$ between RDWC$_U$ and column C3 with HI con-

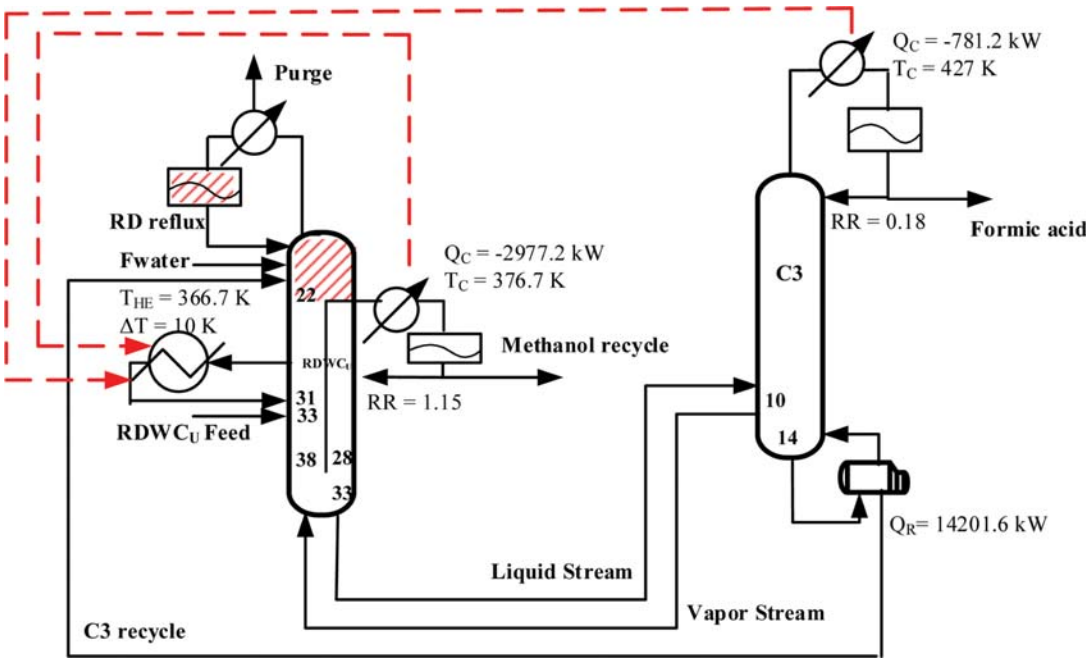

Fig. 20. Flowsheet for the configuration of the NRDWC$_U$ between RDWC$_U$ and column C3 with HI.

Table 2. Comparison of all configurations with external HI arrangement

		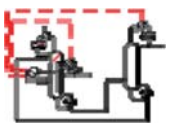	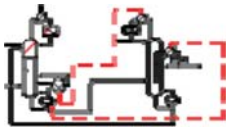	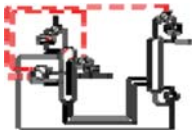
RD reboiler duty (kW)	8495.6	-	4981.9	-
C2 reboiler duty (kW)	4578.2	10320.5	-	-
C3 reboiler dury (kW)	1602.7	2423.9	5843.4	14201.6
Total duty (kW)	14676.5	12744.4	10825.3	14201.6
Energy saving (%)	28.0	37.5	**46.9**	30.3

figuration could only save 13.2% and 3.24% of energy, respectively.

On comparison of the configurations with HI arrangement with those without HI arrangements, the configuration with the $RDWC_U$ between the RD column and column C2 could save 31.8% of the energy using HI arrangement. Then, around 48.5% and 18.55% of energy could be saved through the proposed configuration with the $NRDWC_U$ between columns C2 and C3 with HI arrangement and that with the $NRDWC_U$ between $RDWC_U$ and column C3 with HI configuration, respectively.

These results showed that the HI arrangement had the greatest influence in terms of energy efficiency. Moreover, a larger recycle flow rate in DWC arrangement appeared to contribute to the energy saving. The simulation results obtained in this study revealed the potential of one DWC arrangement, which was better than that of a double-DWC arrangement, and the potential of a configuration with external HI combined with DWC in enhancing the energy efficiency of the high-purity FA production process.

CONCLUSIONS

High-purity FA is an important chemical that finds use in pharmaceuticals/food chemicals and many other applications. Several proposed configurations have been examined in this study to find the best configuration for high-purity FA production. A patented configuration using RD column was optimized for use as the base case. The effects of several main process variables were investigated via a mesh search method to find the optimal base case with the lowest energy requirement. Then, the DWC and external HI arrangements were applied to the conventional base case configuration. Eight configurations were proposed using conventional, DWC, and external HI arrangements. The configurations that combined DWC and external HI offered greater advantages than the DWC alone did. The one-DWC arrangement was found better than the double-DWC arrangement for high-purity FA production. As a result, the best plantwide design for the high-purity FA production process was considered to include the $NRDWC_U$ between columns C2 and C3 with HI configuration, which could save 46.9% energy compared to the conventional base case without HI configuration.

ACKNOWLEDGEMENTS

This study was supported by the 2016 Yeungnam University Research Grant.

NOTES

The authors declare no competing financial interest.

REFERENCES

1. Ihs.com, 2013, Formic acid chemical economics handbook, [online] Available from: http://www.ihs.com/products/formic-acid-chemical-economics-handbook.html (Accessed 26.06.16).
2. Marketsandmarkets.com, 2016, Formic acid market worth $618,808.7 Thousand by 2019, [Online] Available from: http://www.marketsandmarkets.com/PressReleases/formic-acid.asp (Accessed 26.06.2016).
3. J. D. Leonard, US Patent, 4,299,981 (1981).
4. H. P. Huang, M. J. Lee, H. Y. Lee and J. H. Chen, US Patent, 0123157 A1 (2012).
5. C. Tsouris and J. V. Porcelli, *Chem. Eng. Prog.*, **99**, 50 (2003).
6. F. J. Novita, H. Y. Lee and M. Lee, *Chem. Eng. Processing: Process Intensification*, **97**, 144 (2015).
7. M. M. Sharma and S. M. Mahajani, in *Reactive distillation: status and future directions*, K. Sundmacher, A. Kienle Eds., Wiley-VCH Verlag CmbH & Co., KGaA (2002).
8. H. Yoo, M. Binns, M. G. Jang, H. Cho and J. K. Kim. *Korean J. Chem. Eng.*, **33**, 405 (2016).
9. S. H. Lee, M. Shamsuzzoha, M. Han, Y. H. Kim and M. Lee, *Korean J. Chem. Eng.*, **28**, 348 (2011).
10. N. V. D. Long and M. Lee, *Korean J. Chem. Eng.*, **29**, 567 (2012).
11. S. Y. Kim, D. M. Kim and B. Lee. *Korean J. Chem. Eng.*, **34**, 1310 (2017).
12. J. A. Caballero and I. E. Grossmann, *Ind. Eng. Chem. Res.*, **45**, 8454 (2006).
13. M. A. Schultz, D. G. Stewart, J. M. Harris, S. T. Rosenblum, M. S. Shakur and D. E. O'Brien, Reactions and Separations (2002), https:/www.cepmagazine.org.
14. I. Mueller and E. Y. Kenig, *Ind. Eng. Chem. Res.*, **46**, 3709 (2007).
15. G. Bumbac, A. E. Plesu and V. Plesu, *17th European symposium on computer aided process engineering-ESCAPE17* (2007).
16. F. J. Novita, H. Y. Lee and M. Lee, *Ind. Eng. Chem. Res.*, **56**, 7037 (2017).
17. W. Luyben, *Distillation design and control using aspen simulation*, Wiley, Hoboken, NJ (2006).
18. L. Bai, Y. L. Zhao, Y. Q. Hu, B. Zhong and S. Y. Peng, *J. Nat. Gas Chem.*, **5**, 229 (1996).

19. C. X. Wang, *J. Chem. Eng.*, **6**, 898 (2006).
20. J. Polak and B. C. Y. Lu, *J. Chem. Thermodyn*, **4**, 469 (1972).
21. A. Reichl, U. Daiminger, A. Schmidt, M. Davies, U. Hoffmann, C. Brinkmeier, C. Reder and W. Marquardt, *Fluid Phase Equilib.*, **153**, 113 (1998).
22. J. Zeng, Z. Y. Zhu and W. L. Hu, *Nat. Gas Chem. Ind.*, **6**, 56 (2000) (in Chinese).
23. T. Ito and F. Yoshida, *J. Chem. Eng. Data*, **8**, 315 (1963).
24. T. Pöpken, L. Götze and J. Gmehling, *Ind. Eng. Chem. Res.*, **39**, 2601 (2000).

APPENDIX

A1. Kinetic of the Carbonyl Reaction

The kinetic equation of the carbonyl reaction can be found in Bai et al.'s work [18]. The kinetic rate of the carbonyl reaction is represented by

$$r_{carbonyl}=(1.414\times10^{9})\exp(-70748/RT)[cat]_L[MeOH]_L[CO]_L - (2.507\times10^{12})\exp(-92059/RT)[cat]_L[MF]_L \quad (A\text{-}1)$$

where $r_{carbonyl}$ is kinetic rate of carbonyl reaction (mol/L·min), R is the universal gas constant (R=8.314 J·mol^{-1}·K^{-1}), T is the reaction temperature (K), the subscript L indicates the liquid phase concentration (mol/L) and $[CO]_L=[CO]_G=0.154\ P_{CO}/RT$.

A2. Kinetic of the Hydrolysis Reaction

The kinetic model for the MF hydrolysis reaction is given as proposed by Wang [19]:

$$r_{hydrolysis}=\frac{6.530\times10^{6}}{1+0.0869\ [H2O]^{2}} \exp\left(-\frac{63100\ kJ\cdot mol^{-1}}{RT}\right)\left(\frac{[H2O][MF]-[MeOH][FA]}{0.4492\exp(-251/T)}\right) \quad (A\text{-}2)$$

where $r_{hydrolysis}$ is kinetic rate of hydrolysis reaction (kmol·h^{-1}·kg^{-1} (cat)), R is the universal gas constant (R=8.314 kJ·kmol^{-1}·K^{-1}), T is the reaction temperature (K), and [ ] indicates the component concentration (kmol·m^{-3}). Note that it was assumed the correct kinetic rate of the hydrolysis reaction unit is kmol·h^{-1}·kg^{-1}(cat) and the catalyst density is 3,600 kg/m^3.

A3. Thermodynamic Model

Several pairing parameters were obtained through the model regression of the experimental data, such as those obtained by Polak and Lu [20], Reichl et al. [21], Zeng et al. [22], Ito and Yoshida [23], and Pöpken et al. [24], who obtained the pairing parameters for the MeOH-MF, MF-water, MF-FA, water-FA, and MeOH-water systems, respectively. The UNIFAC model was used to estimate the missing parameter for the methanol-FA system. Table A1 shows the UNIQUAC model parameters used in this FA production process.

Table A1. UNIQUAC model parameters used in this study

i	(1)	(1)	(1)	(2)	(2)	(3)
j	(2)	(3)	(4)	(3)	(4)	(4)
a_{ij}	0	0	1.46	2.06	0.65	0
a_{ji}	0	0	1.86	−3.15	4.99	0
b_{ij}	−434.24	−15.20	−471.54	−219.04	−155.34	366.61
b_{ji}	−99.35	−301.76	132.65	575.68	−1802.30	−615.90
d_{ij}	0	0	0	−0.007	0	0
d_{ji}	0	0	0	0.006	0	0

*Note: (1) MF, (2) H_2O, (3) MeOH, (4) FA